

Optical properties of metals: Infrared emissivity in the anomalous skin effect spectral region

T. Echániz,¹ R. B. Pérez-Sáez,^{1,2,a)} and M. J. Tello^{1,2}

¹*Departamento de Física de la Materia Condensada, Facultad de Ciencia y Tecnología, UPV/EHU, Sarriena s/n, Leioa 48940, Spain*

²*Instituto de Síntesis y Estudio de Materiales, Universidad del País Vasco, Apdo. 644, Bilbao 48080, Spain*

(Received 25 June 2014; accepted 18 August 2014; published online 4 September 2014)

When the penetration depth of an electromagnetic wave in a metal is similar to the mean free path of the conduction electrons, the Drude classical theory is no longer satisfied and the skin effect becomes anomalous. Physical parameters of this theory for twelve metals were calculated and analyzed. The theory predicts an emissivity peak ε_{peak} at room temperature in the mid-infrared for smooth surface metals that moves towards larger wavelengths as temperature decreases. Furthermore, the theory states that ε_{peak} increases with the emission angle but its position, λ_{peak} , is constant. Copper directional emissivity measurements as well as emissivity obtained using optical constants data confirm the predictions of the theory. Considering the relationship between the specular parameter p and the sample roughness, it is concluded that p is not the simple parameter it is usually assumed to be. Quantitative comparison between experimental data and theoretical predictions shows that the specular parameter can be equal to one for roughness values larger than those predicted. An exhaustive analysis of the experimental optical parameters shows signs of a reflex Au, and Mo around the wavelength predicted by the theory for $p = 1$.

I. INTRODUCTION

The skin effects in metals are some of the fundamental problems of physical kinetics and have received attention because of their many possible applications. For example, a great number of advanced optoelectronic devices use high reflectivity mirrors with a very stable surface. These conditions are satisfied by bulk metal mirrors and thin and thick metallic films deposited on active or passive substrates. In these applications, it is necessary to know the optical conductivity $\sigma(\omega)$ and either the complex refractive index $\tilde{n}(\omega)$ or the complex dielectric function $\tilde{\epsilon}(\omega)$. These physical parameters are temperature and wavelength dependent. Besides, the use of metal mirrors requires obtaining accurately the amplitude and the phase of the reflection coefficient of these optical devices. The change of phase in the visible and infrared range is a function of the wavelength and can be calculated if $\tilde{n}(\omega)$ and $\sigma(\omega)$ are known. These and other optical and electrical applications justify the effort made in the measurement of the optical properties of metals. These optical magnitudes are usually deduced from the measurement of some observable using reflectivity, transmission, absorption, ellipsometry, light scattering, or dielectric measurements. At this time, most of the accessible optical experimental data are compiled in tables in several publications.¹⁻⁵ Unfortunately, the measurements of these observables for metals present serious difficulties for energies below 1 eV since the reflectivity of a great number of metals is very close to 1 for those energies. The difficulty to find reliable data increases for temperature dependent measurements as

well. This is the reason why in the literature little experimental data can be found for $\lambda > 10\mu\text{m}$. It has been recently shown that at least above room temperature the emissivity $\varepsilon(\omega, \theta)$ can be used.⁶ This parameter is equivalent to the normal incident reflectivity, $R(\omega, \theta)$, as $\varepsilon = 1 - R$, assuming that $T = 0$ (T is the transmitted light fraction). In addition, it should be noted that the comparison between infrared experimental optical data is complicated because the instrumental difficulties and the optical constant measurements are very sensitive to the quality of the sample surface: roughness, surface cleaning, surface flatness, thermal history, etc. Another fact to consider is that the values of the optical constants of thin films differ from the ones measured in thick layers and bulk metals. Furthermore, in the case of very thin films the values of optical and electrical parameters depend on the film thickness.

Some metals have an infrared spectral region, in which the classical Drude theory is no longer valid due to the fact that the conduction electrons mean free path length has the same order of magnitude as the amplitude of the penetration depth of the electromagnetic field. In this region, the normal skin effect transforms into the anomalous skin effect. This effect was incorporated into the general theory of the optical properties of metals in connection with its electronic structure with the first theoretical papers published by Pippard, Reuter and Sondheimer, Dingle, and others.⁷⁻¹⁴ For the reasons given earlier about the difficulties of infrared metal optical measurements and because the anomalous region extends above $100\mu\text{m}$, it follows that an experimental effort to allow a better comparison with theoretical predictions is very interesting. The purpose of this paper is to confirm that a significant number of metals, many of them used in

^{a)}raul.perez@ehu.es

optoelectronic applications, present an anomalous skin effect in the mid and far-infrared spectral region. Using all the literature accessible experimental data of optical constants together with emissivity measurements of our laboratory, we can check that, in agreement with the theory of the anomalous skin effect, copper shows an emissivity broad peak in the mid-infrared at room temperature. A quantitative comparison between experimental data and theoretical predictions together with a discussion about the specular parameter and the surface roughness are carried out.

II. BACKGROUND

In most metal optical applications (e.g., metal mirrors), it is necessary to know the response of the electrons to the incident electromagnetic field. Depending on the frequency this response is related to the intraband transitions of the conduction electrons, the interband transitions due to internal photoelectric effect or both of them. Other absorption mechanisms, such as lattice absorption and localized states, should only be considered in specific frequency ranges. For a large portion of the infrared spectrum, the interband transitions are forbidden for the metals analyzed in this paper. In this spectral region, the absorption mechanism is associated to intraband transitions. Assuming that other possible absorption effects such as electron-electron or multiple phonon processes are negligible, the interaction is described by means of the relation between the current density and the electrical field in the metal. This relationship requires solving the relaxation time approximation Boltzmann equation for the non-equilibrium part of the electron distribution function. This equation contains a diffusion term that can be omitted when the electric field inside the metal can be considered spatially constant. This assumption is valid when

$$\frac{l}{\delta} \ll \frac{(1 + (\omega\tau)^2)^{\frac{3}{4}}}{(\omega\tau)^{\frac{1}{2}}}, \quad (1)$$

where l is the electron mean free path and the penetration depth $\delta(\omega)$ of the electromagnetic field for optical frequencies is given by

$$\delta(\omega) = \text{Re} \left[\frac{c(1 + i\omega\tau)^{\frac{1}{2}}}{(2\pi\sigma_0\omega)^{\frac{1}{2}}(1 + i)} \right], \quad (2)$$

where σ_0 is the dc conductivity and τ is the relaxation time. In many papers, the penetration depth is obtained using a simplified formula $\delta_0^2 = 2c^2/\omega_p\omega\tau$, where $\omega_p^2 = 4n_e e^2\pi/m^*$ is the plasmon frequency of conduction electrons. In this case, the calculated penetration depth value may differ from those found with Eq. (2) by a factor that can be as high as 4. Other physical parameters used in the theoretical calculus are

$$n_e = \frac{8\pi}{3} \left(\frac{mv_F}{h} \right)^3, \quad \sigma = \frac{n_e e^2 l}{mv_F}, \quad l = v_F \tau, \quad \alpha = \frac{3}{2} \left(\frac{l}{\delta} \right)^2$$

$$\beta = \frac{\alpha}{\omega\tau}, \quad \zeta = \frac{i\alpha}{(1 + i\omega\tau)^3}, \quad m \approx m^*, \quad (3)$$

where n_e is the electron density, v_F is the Fermi velocity, m^* is the electron effective mass, ζ is a parameter that takes into account the relative sizes of the energy loss mechanisms, and α and β are coefficients used in the theory. If Eq. (1) is satisfied, the interaction between the electromagnetic field and the metal is called normal skin effect. At low and high infrared frequencies ($\omega\tau \ll 1$ and $\omega\tau \gg 1$), the inequality will hold regardless of the value of τ and σ_0 and the experimental results must be in reasonably good agreement with the classical Drude theory.¹⁵ The emissivity can be obtained using the classical equation

$$\varepsilon(\omega) = \frac{4n}{(n+1)^2 + k^2}, \quad (4)$$

where the refractive index n and the extinction coefficient k are obtained from the following equations:

$$n^2 - k^2 = 1 - \frac{4\pi\sigma_0\tau}{(\omega\tau)^2 + 1}, \quad nk = \frac{4\pi\sigma_0\tau}{\omega\tau((\omega\tau)^2 + 1)}. \quad (5)$$

At mid and far-infrared frequencies, Eq. (1) may not be satisfied even above room temperature. It is a wide region, with $l \approx \delta$, where the Drude classical theory is not valid, and it is called the anomalous skin effect spectral region. In this case, the dependence of the optical properties with the conduction electrons must take into account the non-local character of the relationship between the field and current density which forces to retain the diffusion term in the Boltzmann equation. Since the first paper about a phenomenological approach of the anomalous skin effect,⁹ a major effort to complete the theory as well as to find experimental confirmation has been done. The theoretical approaches^{8,9} express the metal optical properties in terms of the surface impedance $Z = R + iX$ (where R is the surface resistance and X is the surface reactance). From the surface impedance, the reflectance and the emissivity as a function of relaxation time and optical conductivity can be obtained.

In most of the papers, the experimental results are compared with two sorts of semiclassical equations for the theoretical surface impedance. Those that take the form of definite integrals solved numerically^{8,16,17} and those where the surface impedance is obtained from series expansions.^{9-11,18} Even though we will make use of integral equations a comparison with theoretical predictions of the series expansions will be displayed. Besides, the quantum mechanical derivation,^{6,7} for temperatures above the Debye temperature, gives the same surface impedance equations. We shall not give here details of the calculations performed by Pippard, Reuter and Sondheimer, and Dingle.⁸⁻¹¹ Furthermore, the model assumes that a fraction p ($0 \leq p \leq 1$) of the electrons arriving at the surface is scattered specularly, while the rest are scattered diffusely.¹⁹ However, other possible assumption will be discussed later on this paper. In any case, considering the experimental results, we will only consider the theoretical equations corresponding to $p = 1$. Also, the theoretical approach used ignores the displacement current, which is not relevant in the mid-infrared for the metals in Table I. For the optical region, the emissivity is given by⁶⁻⁸

TABLE I. Physical parameters of the metals that according to Eq. (1) must present an anomalous skin effect spectral region at room temperature. τ is the relaxation time, n_e is the carrier density, ω_p is the plasmon frequency, σ is the dc conductivity, ρ is the dc resistivity, l is the mean free path, and v_F is the Fermi velocity. The rest of the parameters show the strength of the anomalous skin effect on the optical properties and those with an asterisk are calculated for $\lambda = \lambda_{max}$.

Element	Ag	Cu	Au	Ca	Al	Rh	Mg	Mo	Ir	W	Zn	Ru
τ (fs)	38.2	25.2	27.1	22.9	7.2	10.9	9.4	10.6	4.8	5.1	4.5	6.4
n_e (10^{22} cm $^{-3}$)	5.86	8.47	5.90	4.61	18.07	7.26	8.61	6.41	14.12	12.64	13.14	7.27
ω_p (10^{16} Rad/s)	1.37	1.64	1.37	1.21	2.40	1.57	1.66	1.43	2.12	2.01	2.05	1.52
σ (10^{17} esu)	5.67	5.36	4.05	2.67	3.30	2.00	2.05	1.71	1.70	1.64	1.50	1.18
ρ (10^{-8} Ω m)	1.59	1.68	2.21	3.36	2.82	4.49	4.66	5.23	5.29	5.49	5.95	7.60
l (10^{-6} cm)	5.31	3.93	3.78	2.94	1.46	1.62	1.49	1.52	0.90	0.92	0.82	0.96
v_F (10^8 cm/s)	1.39	1.57	1.39	1.28	2.03	1.49	1.58	1.43	1.87	1.80	1.82	1.50
β	4.39	3.47	2.24	1.06	1.02	0.51	0.51	0.39	0.30	0.28	0.23	0.18
λ_{max} (μ m)	31.3	21.5	25.5	24.3	7.7	12.6	11.0	12.7	5.8	6.3	5.6	8.2
$(\epsilon/\epsilon_{clas})_{max}$ (%)	21.6	18.3	13.2	7.5	7.2	4.1	4.1	3.3	2.6	2.5	2.1	1.7
$\omega\tau$ (*)	2.30	2.19	2.00	1.77	1.76	1.63	1.61	1.57	1.55	1.53	1.51	1.48
δ_{clas} (10^{-6} cm) (*)	2.05	1.75	2.19	2.62	1.33	2.19	2.01	2.37	1.61	1.71	1.69	2.29
ξ (*)	0.64	0.55	0.40	0.22	0.22	0.12	0.12	0.10	0.07	0.07	0.06	0.05
λ_{peak} (μ m)	27.3	18.3	20.5	17.2	5.4	7.1	6.2	6.3
ϵ_{max}	0.0046	0.0057	0.0060	0.0076	0.0121	0.0123	0.0130	0.0134

$$\epsilon(\omega) = \epsilon_{clas} \frac{4c}{\pi^2} \sqrt{\frac{2\alpha}{3}} \frac{\omega\tau \text{Re}[I] - \text{Im}[I]}{1 + \omega^2\tau^2 \sqrt{-\omega\tau + \sqrt{1 + \omega^2\tau^2}}}, \quad (6)$$

where ϵ_{clas} is the classical emissivity and

$$I = \int_0^\infty \frac{dz}{z^2 + \xi k(z)}, \quad (7)$$

where $k(z)$ is a function of z (perpendicular distance to the metal surface)

$$k(z) = \frac{2}{z} [(1 + z^2)\arctan z - z]. \quad (8)$$

The series expansion of the surface impedance used in the paper⁹ is

$$-i \frac{(1 + i\omega\tau)c^2}{4\pi\omega\tau v_F} Z = 0.7698(\pi\xi)^{-\frac{1}{3}} + 0.6534(\pi\xi)^{-\frac{2}{3}} + \dots, \quad (9)$$

and for near and mid-infrared it can also be used

$$-i\omega Z = \frac{\sqrt{3}}{2} \xi^{-\frac{1}{2}} + \frac{\sqrt{3}}{15} \xi^{\frac{1}{2}} - \frac{1}{6} \xi + \dots \quad (10)$$

As already indicated, the anomalous skin effect theory⁷⁻⁹ involves a reflectivity parameter p that takes into account the effect of the physical surface on electron transport in metals and semiconductors.¹⁹ The value of this parameter, which is not known *a priori*, is between $p=1$ assuming complete specularity and $p=0$ for complete diffuseness. From an experimental point of view, this parameter is related to the surface roughness and has been extensively discussed in the literature.²⁰⁻²⁸ Using the de Broglie wavelength of electrons as well as the roughness value is possible to find when the surface loses its specular character and therefore when to use the theoretical formulas with $p=0$ instead of those with $p=1$. However, in a great number of papers about optical properties of metals, semimetals, and

semiconductors $p=0$ is obtained for both specular and diffuse surfaces.¹⁶⁻²⁸ This means that the surface roughness value for which is assigned complete diffuseness ($p=0$) cannot be the same as that obtained from diffraction theory. Furthermore, it is easy to see that even with the interpretation of the parameter p indicated, its value expressed in terms of probabilities of scattering is different from that of the kinetic probability of specular reflection.²⁸ This analysis shows that $p=1$ for a metal does not necessarily imply that the metal surface is smooth compared with the de Broglie wavelength.²⁰ This conclusion, which has an experimental demonstration in this article, indicates that many interpretations have assumed $p=0$ for a roughness value that is related to $p=1$ or an intermediate value.

Fig. 1 shows theoretical spectral emissivity for the classical theory (Eq. (4)) and for the anomalous skin effect with $p=1$ (Eq. (6)) at three temperatures. It must be noticed that the anomalous skin effect normal emissivity shows, for $p=1$, a broad peak in the mid and far-infrared spectrum. Among the metals that have an anomalous skin effect behavior, listed in Table I, only copper⁶ shows a clear experimental confirmation of an emissivity broad peak in the mid-infrared in agreement with the theoretical predictions. In the same figure, the two series expansion approximations (Eqs. (9) and (10)) are also plotted. The plots confirm the range of validity of both equations. Thus, Eq. (9) is a better approximation for higher temperatures, while Eq. (10) works better for lower ones. In the same figure, the expansion series emissivity for $p=0$ is also plotted. Two facts should be outlined: on the one hand, the strong dependence of the anomalous skin effect with temperature; on the other, it is better to use the integral equation because the series expansion approach only covers a fraction of the anomalous wavelength range.

III. EXPERIMENTAL

Copper emissivity measurements between 3 and 24 μ m were carried out with the homemade HAIRL radiometer²⁹

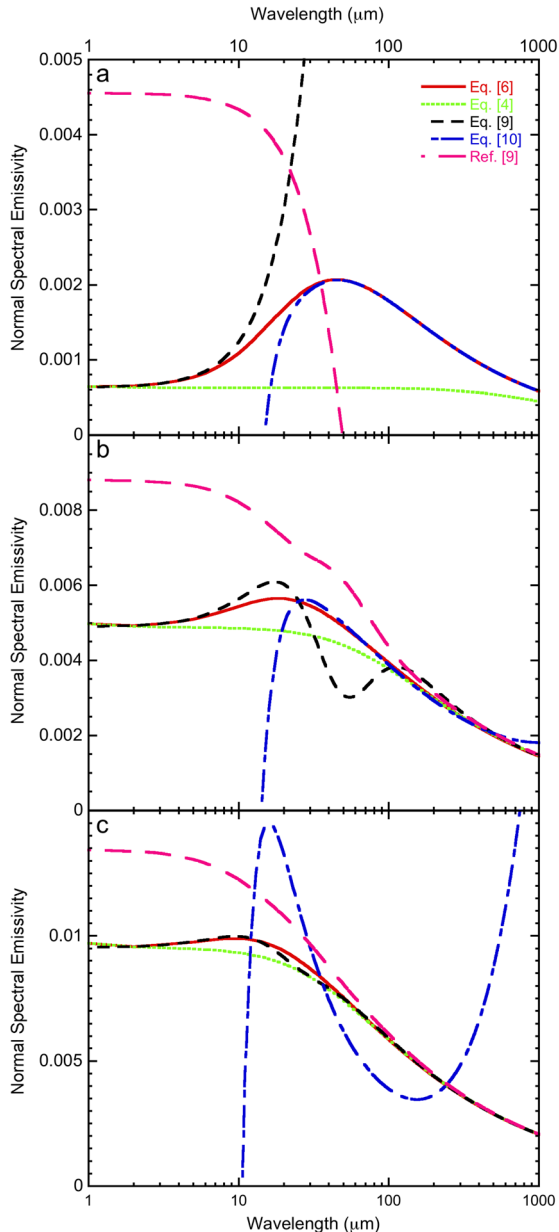


FIG. 1. Classical and anomalous skin effect emissivities given by Eq. (4) (dotted, green), Eq. (6) (solid, red), Eq. (9) (dashed, black), Eq. (10) (dotted-dashed, blue) and series expansion for $p=0$ (long-dashed, pink).⁹ (a) $T = 80$ K, (b) $T = 293$ K, and (c) $T = 526$ K. The physical parameters used are those for copper in Table I.

that allows an accurate detection of the thermal radiation as well as its fast processing. The sample chamber ensures a controlled atmosphere and allows directional measurements. Direct spectral emissivity measurements were made using the blacksurr method,³⁰ and the calibration was carried out using a modified two-temperature method.³¹ The combined standard uncertainty is obtained from the analysis of all uncertainty sources.³² The experimental uncertainty varies with the wavelength, with 2% at $4\mu\text{m}$ and 12% at $16\mu\text{m}$.

The measurements were carried out on electrolytic copper thick films (thickness $>36\mu\text{m}$) placed on 6 cm diameter iron discs. The surface roughness values were: $1.05 < R_a < 1.26\mu\text{m}$. For each sample, four previous thermal cycles were performed up to 800°C . This thermal treatment ensures

that the possible presence of surface stress is completely removed.^{33,34} Finally, X-Ray diffraction and electron microscopy were used to check the absence of sample surface oxidation and contamination.

IV. RESULTS AND DISCUSSION

Table I lists the metals that according to Eq. (1) must present an anomalous behavior in the infrared region at room temperature, together with most part of the physical magnitudes that are used in the theoretical calculations of this paper. Literature bulk metal experimental data (n , τ , σ , v_F , and l)^{15,35} were used to obtain the other physical parameters in Table I. It can be checked that the penetration depth of the metals listed in the table satisfies the anomalous skin effect condition $l \approx \delta$. It can also be observed that the plasmon frequency lies in the ultraviolet spectral region and is similar for all metals with anomalous skin effect. The order in which the metals are listed in Table I is based on the value of the strength of the anomalous behavior for each metal (β and ζ). Moreover, two wavelengths whose values can be compared with the experimental results are shown. λ_{peak} is the wavelength at which the anomalous skin effect emissivity goes through a maximum (ε_{max}). λ_{max} is the wavelength at which the percentage of the anomalous skin effect emissivity compared to the Drude (classical) theory emissivity is maximum $(\varepsilon/\varepsilon_{clas})_{max}$. As it should be, the values of $(\varepsilon/\varepsilon_{clas})_{max}$ for each metal show the same sequence as that of β and ζ . Furthermore, only two of the parameters need to be obtained from experimental data since the rest can be obtained by using Eqs. (3) and (6). In our case, the two parameters obtained from the literature where the electric resistance ρ and the carrier density n_e .

Equations (4)–(6) and the parameters of Table I allow to obtain the theoretical predictions of the wavelength dependence of the classical and anomalous skin effect emissivities for any temperature. In Fig. 2, the room temperature theoretical emissivities of the first five metals from Table I are shown for comparison. In the anomalous skin effect region, the emissivity of the five metals shows a broad peak in the

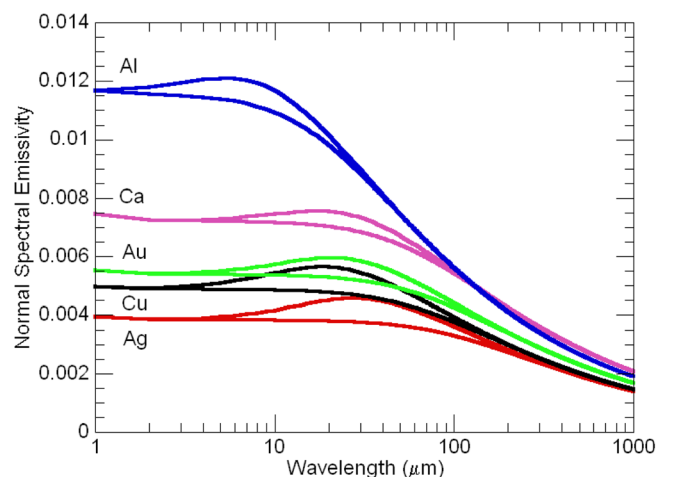


FIG. 2. Predicted classical (Eq. (4)) and anomalous skin effect emissivities (Eq. (6)) of five metals at room temperature.

mid-infrared at room temperature. Similar results are obtained for the other metals in Table I. According to Table I, the highest values for $(\varepsilon/\varepsilon_{clas})_{max}$, λ_{max} , and λ_{peak} correspond to silver. A first conclusion can be stated: the anomalous skin effect theory predicts that all metals in Table I exhibit the unusual anomalous skin effect, at room temperature and $p = 1$. Therefore, its emissivity must show a broad peak in the mid-infrared.

At low temperature, the emissivity broad peak is shifted to larger wavelengths, $(\varepsilon/\varepsilon_{clas})_{max}$ grows and the anomalous skin effect spectral range is larger, while at higher temperatures, λ_{peak} is shifted to shorter wavelengths and the relative value of $(\varepsilon/\varepsilon_{clas})_{max}$ as well as the anomalous skin effect range decreases. This theoretical prediction is particularized for copper in Fig. 3. The relative emissivity $(\varepsilon/\varepsilon_{clas})_{max}$ value changes from 330% at 80 K to 7% at 526 K and the anomalous skin effect spectral range changes from $\Delta\lambda \approx 1000\mu\text{m}$ for 80 K to $\Delta\lambda \approx 50\mu\text{m}$ for 526 K. In any case, it must be remembered that the emissivity calculated from Eqs. (6), (9) or (10) is very sensitive to the values of the relaxation time, or, equally, the conductivity data. Small changes in the value of these experimental parameters may lead to noticeable differences on λ_{peak} and λ_{max} .

Within our knowledge all literature tables and papers about optical and dielectric constants, as well as reflectance and emissivity measurements of the listed metals in Table I, are analyzed. An emissivity broad peak in the mid-infrared or, at least, an indication that the peak can exist was only found for Cu, Al, Au, and Mo.^{5,6,36-38} In any case, the refractive indexes were usually measured for $\lambda < \lambda_{peak}$, and in most cases, the surface characterization is not specified and the experimental errors, which are not given, could be large. Even using a good reflectometer,²⁰ measurements of the infrared optical constants of metals offer serious difficulties. This can be extended to other experimental devices³⁹ and explains the little experimental data above $10\mu\text{m}$ and its large scatter making it difficult to detect the small variations associated to the anomalous skin effect at room temperature.

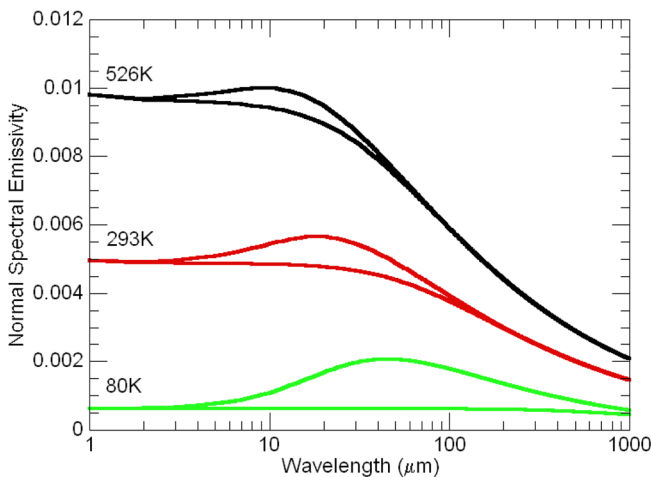


FIG. 3. Predicted classical (Eq. (4)) and skin anomalous effect emissivities (Eq. (6)) of copper at three temperatures.

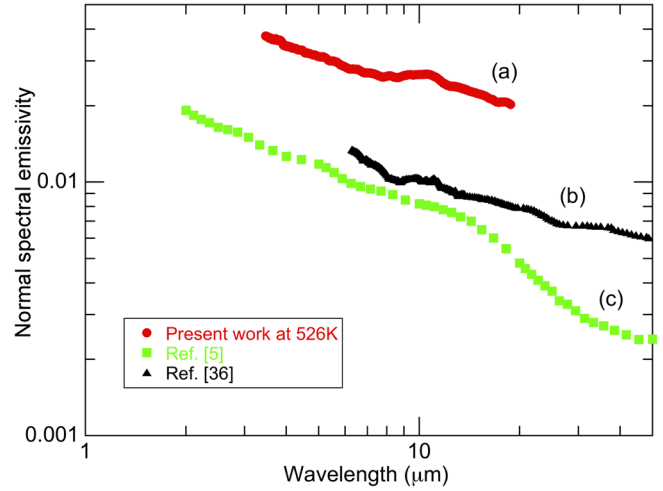


FIG. 4. Copper normal spectral experimental emissivity $\varepsilon(\lambda, T)$: (a) from radiometric measurements at 526 K; (b) from room temperature reflectivity measurements;³⁶ and (c) from Eq. (4) using experimental optical constants.⁵

Fig. 4 shows three copper emissivity experimental results as a function of the wavelength. Curve (a) corresponds to normal spectral experimental emissivity measurements carried out in our laboratory at 526 K. Curve (b) was obtained from literature reflectivity data³⁹ at room temperature and curve (c), also at room temperature, was obtained using Eq. (4) with literature optical constant data.⁵ The curves show evidences of the emissivity broad peak associated to the anomalous skin effect. In the case of curve (a), a broad peak is observed around $10\mu\text{m}$, a broad shoulder is observed in curve (c) around $16\mu\text{m}$, whereas in curve (b), one can consider that it shows a broad peak between 9 and $29\mu\text{m}$. Since finding the position of the maximum in curve (b) is not easy, curves (a) and (c) will be the only ones used. Taking into account that ε_{clas} cannot be obtained experimentally, the experimental λ_{max} is obtained from $(\varepsilon/\varepsilon_{baseline})_{max}$, where $\varepsilon_{baseline}$ is the experimental curve baseline that replaces ε_{clas} . These baselines cannot be obtained very precisely (in our case a straight line replaces the peak), and therefore this approach leads to differences between experimental and theoretical values, which also depend on the spectral range of the experimental measurements. As a consequence, it is better to use λ_{peak} , whose values at room temperature are in good agreement with the theoretical prediction for those temperatures ($17.4\mu\text{m}$ and $9.4\mu\text{m}$, respectively).

The broad peak in the three copper emissivity curves in Fig. 4 together with the similar peaks for Al,³⁶ Au,³⁷ and Mo (Ref. 38) are an experimental evidence that at least these four metals show a behavior in agreement with the predictions of the semiclassical theory of anomalous skin effect for $p = 1$. As indicated before, the parameter p introduced in the anomalous skin effect theory has a simple boundary condition which in terms of distribution function is written as $f(v) = pf(-v)$,¹⁹ where f is the distribution function for incident and reflected conduction electrons. This boundary condition entails that $p = 1 - W_s$, where W_s is the probability that an electron can be diffusely scattered. The qualitative agreement between Eq. (6) with experimental results (Fig. 4) shows that, according to the boundary condition used in

Eq. (6), W_s should be approximately zero. This probability can be calculated using diffraction theory. Considering electrons as a non-degenerate system, it was found that the surface must be nearly atomically smooth for specular electronic reflection to occur.²⁰ However, the sample surfaces in Fig. 4 have high roughness, particularly those that have been used in the direct normal emissivity measurements. The values obtained should fit with $p=0$ but they do it much better with $p=1$. This result indicates that p is not the simple parameter that it is usually assumed to be.

The experimental results in Fig. 4 seem to be in agreement with a more general electron gas boundary condition²⁸ that leads to a new current equation with bulk and surface contributions. In particular, the surface contribution contains two terms associated to the outgoing flux in a particular direction: the specularly reflected electrons and the diffuse ones whose angular distribution depends on the detailed scattering mechanisms at the surface. This means that in degenerate systems an additional weighting factor appears. For this reason, p can be nearly 1, even when the restricted boundary condition gives $1 - W_s = 0$. Thus, the specularity is present in surfaces with larger roughness values than those predicted by the W_s calculus. Therefore, there is a higher maximum roughness value than the one predicted by the diffraction theory. In addition, the roughness does not only affect the functional form of the parameter p but also modifies the absolute value of the emissivity.⁴⁰ If the sample has a roughness $r < r_{max}$, the general boundary conditions allows $p=1$ in the semiclassical theory and the experimental results in Fig. 4 must have the same qualitative behavior. However, a quantitative agreement is not possible since the experimental data (absolute value) depends on the roughness value. It is interesting to recall that for a given roughness the reflectivity rises as wavelength increases because the surface is relatively smoother to the incident radiation. This explains not only the differences in the absolute values of emissivity but also the slope differences between the experimental data in the literature and the results obtained with theoretical predictions.

Besides, other considerations must be taken into account. The conventional emissivity concept implies that thermal emission is a surface phenomenon. However, thermal radiation emission is a volumetric process that can often be approximated as a surface process because only a small portion of the volume below the emitting surface contributes significantly to the emitted spectrum. But when we want to observe very small emissivity changes it is compulsory to take into account a small volumetric portion defined as the critical thickness. Drude emissivity, emissivity in the anomalous skin effect region, and emissivity due to the surface plasmon could show different effective surface roughness. This concept of volumetric process is in agreement with the idea of a current equation with bulk and surface contributions.²⁸

Fig. 5 shows the theoretical and experimental emissivity ratios ($\varepsilon/\varepsilon_{clas}$ and $\varepsilon/\varepsilon_{baseline}$) at 526 K and room temperature, respectively. It should be noted that the room temperature experimental baseline comprises a spectral range of approximately $50\mu\text{m}$ and is reduced to $20\mu\text{m}$ at 526 K. However, the

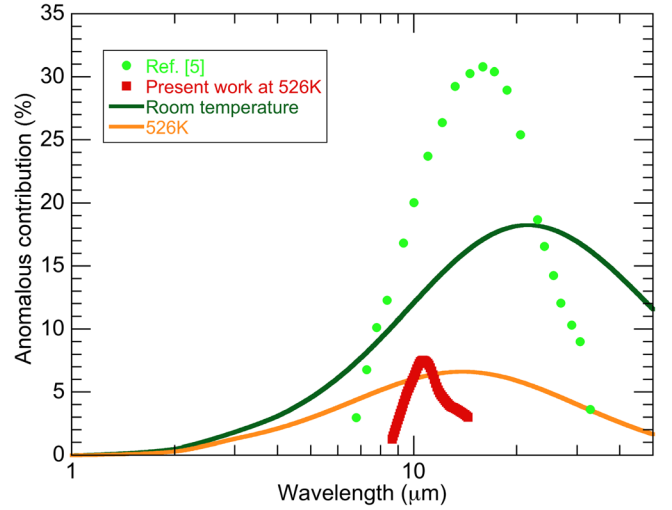


FIG. 5. Theoretical and experimental emissivity ratios $\varepsilon/\varepsilon_{clas}$ and $\varepsilon/\varepsilon_{baseline}$ at 526 K and room temperature.⁵

anomalous region is larger at both temperatures (Fig. 3) and accurate baselines cannot be found due to the experimental limitations. This fact produces important differences between the experimental and the theoretical peak width. The agreement is best at room temperature because the spectral range of these measurements is larger than those at 526 K, and therefore, the experimental baseline is closer to the classical theory prediction. This result is in complete agreement with the influence of roughness on both the theoretical predictions and the quantitative emissivity experimental values. Anyway, more accurate measurements are required in order to see if it is necessary to consider a non-asymptotic approximation^{16,17} of the anomalous skin effect theory. This reformulation predicts the same value for the width of the anomalous skin effect region but a peak value lower than the one predicted by Eq. (6).

Eventually, the semiclassical theory of the anomalous skin effect predicts that the emissivity peak position, λ_{peak} , must be the same for directional and normal measurements. The theoretical curves in Fig. 6 show the copper spectral

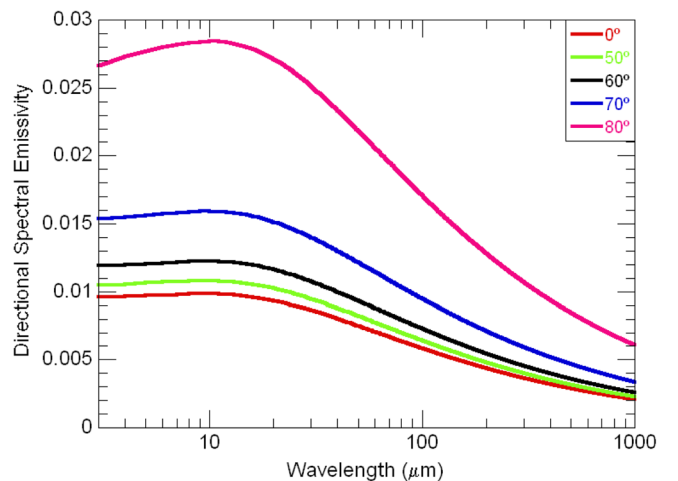


FIG. 6. Theoretical prediction for the directional anomalous skin effect emissivity as function of λ for five different angles at 526 K.

directional emissivity dependence obtained using the semi-classical equations.^{2,17} Here, λ_{peak} , the broad peak width, and $\varepsilon_{peak} - \varepsilon_{clas}$ are the same for the $0^\circ \leq \theta \leq 80^\circ$ emission range. However, the emissivity value rises when the angle increases. This behavior was found in the directional emissivity measurements of copper with non-polarized light.⁶ A good full qualitative agreement between the experimental and the theoretical curves was found. However, we find again quantitative differences in the emissivity values. Here, they are larger than those we saw for normal incidence because as a result of diffraction effects, the directional properties are significantly influenced by the roughness and the parameter p does not take into account this influence. In any case, it is interesting to study the emissivity angular dependence for a fixed wavelength. Fig. 7 provides the experimental and the theoretical copper directional emissivity for three wavelengths. The emissivities are expressed as $(\varepsilon(\lambda, \theta)_{exp} - \varepsilon(\lambda, \theta)_{baseline})$ and $(\varepsilon(\lambda, \theta)_{th} - \varepsilon(\lambda, \theta)_{clas})$. Once again, there is a good qualitative agreement and both are in complete agreement with the predictions of the electromagnetic theory.^{41,42} However, the experimental values are not of the same order of magnitude as the predicted ones. These quantitative differences can be associated with the surface roughness.

In conclusion, a complete literature review of experimental optical constants of twelve metals in the infrared spectral region is presented. According to theoretical predictions these metals have an anomalous skin effect region in the mid and far-infrared at room temperature. Experimental data for Cu, Al, Au, and Mo show signs of a reflectivity broad peak around the wavelength predicted by theory. However, this data does not allow an experimental analysis except for Cu, where the data clearly show the anomalous skin effect for a smooth surface ($p = 1$). In this case, experimental emissivity measurements as well as emissivity obtained using optical constants data confirm the predictions of the theory. In particular, the directional emissivity measurements have revealed that the emissivity value increases

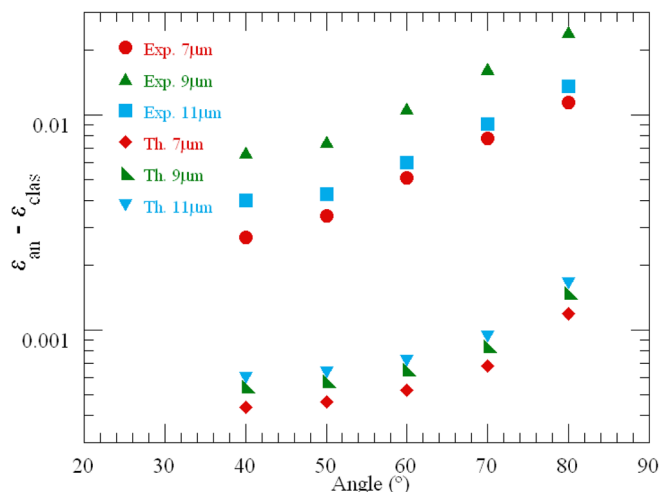


FIG. 7. Experimental and theoretical copper directional emissivity for three wavelengths. The quantitative differences are associated with the surface roughness.

as well as the broad peak position is independent of the emission angle, being both in complete agreement with the electromagnetic theory. Finally, quantitative comparison between experimental emissivity data with theoretical predictions shows that the specular parameter can be equal to one for roughness values larger than those predicted by the diffraction theory. The present results indicate the need to carry out optical measurements in metals in order to study a wider spectral range, reduce the probable errors, and extend measurements at low temperatures.

ACKNOWLEDGMENTS

This research was partially supported by the program ETORTEK of the Consejería de Industria of the Gobierno Vasco in collaboration with the CIC-Energigune Research Center. T. Echániz would like to acknowledge the Basque Government for its support through a Ph.D. fellowship.

- ¹G. Haas and L. Hadley, in *American Institute of Physics Handbook* (McGraw-Hill, New York, 1972), pp. 6–118.
- ²J. H. Weaver *et al.*, in *Physics Data, Optical Properties of Metals* (Fachinformationszentrum 7514 Eggenstein-Leopoldshafen 2, Karlsruhe, Federal Republic of Germany, 1981).
- ³D. W. Lynch and W. R. Hunter, in *Handbook of Optical Constants of Solids*, edited by E. D. Palik (Academic Press, San Diego, 1985).
- ⁴M. A. Ordal, L. L. Long, R. J. Bell, S. E. Bell, R. W. Alexander, Jr., and C. A. Ward, *Appl. Opt.* **22**, 1099 (1983).
- ⁵M. A. Ordal, J. Robert, R. W. Bell, R. W. Alexander, L. L. Long, and M. R. Querry, *Appl. Opt.* **24**, 4493 (1985).
- ⁶T. Echániz, I. Setién-Fernández, R. B. Pérez-Sáez, and M. J. Tello, *Appl. Phys. Lett.* **102**, 244106 (2013).
- ⁷A. B. Pippard, *Proc. R. Soc. A* **191**, 385 (1947).
- ⁸G. E. H. Reuter and E. H. Sondheimer, *Proc. R. Soc. A* **195**, 336 (1948).
- ⁹R. B. Dingle, *Physica* **19**, 311 (1953).
- ¹⁰R. B. Dingle, *Physica* **19**, 348 (1953).
- ¹¹R. B. Dingle, *Appl. Sci. Res. Sec. B* **3**, 69 (1954).
- ¹²D. C. Mattis and J. Bardeen, *Phys. Rev.* **111**, 412 (1958).
- ¹³T. Holstein, *Phys. Rev.* **88**, 1427 (1952).
- ¹⁴M. I. Kaganov, G. Y. Lyubarskiy, and A. G. Mitina, *Phys. Rep.* **288**, 291 (1997).
- ¹⁵N. W. Ashcroft and N. D. Mermin, *Solid State Physics* (Brooks/Cole, Belmont, 1976), Chap. 1.
- ¹⁶K. L. Kliever and R. Fuchs, *Phys. Rev.* **153**, 498 (1967).
- ¹⁷K. L. Kliever and R. Fuchs, *Phys. Rev.* **172**, 607 (1968).
- ¹⁸P. W. Gilberd, *J. Phys. F: Met. Phys.* **12**, 1845 (1982).
- ¹⁹K. Fuchs, *Proc. Cambridge Philos. Soc.* **34**, 100 (1938).
- ²⁰H. E. Bennett, J. M. Bennett, E. J. Ashley, and J. Motyka, *Phys. Rev.* **165**, 755 (1968).
- ²¹M. L. Thèye, *Phys. Rev. B* **2**, 3060 (1970).
- ²²R. F. Greene, *Surf. Sci.* **2**, 101 (1964).
- ²³E. W. Johnson and H. H. Johnson, *J. Appl. Phys.* **36**, 1286 (1965).
- ²⁴J. N. Zemel and R. L. Petritz, *Phys. Rev.* **110**, 1263 (1958).
- ²⁵G. E. Smith, *Phys. Rev.* **115**, 1561 (1959).
- ²⁶K. L. Chopra, L. C. Bobb, and M. H. Francombe, *J. Appl. Phys.* **34**, 1699 (1963).
- ²⁷D. C. Larson and B. T. Boiko, *Appl. Phys. Lett.* **5**, 155 (1964).
- ²⁸R. F. Greene, *Phys. Rev.* **141**, 687 (1966).
- ²⁹L. del Campo, R. B. Pérez-Sáez, X. Esquisabel, I. Fernández, and M. J. Tello, *Rev. Sci. Instrum.* **77**, 113111 (2006).
- ³⁰R. B. Pérez-Sáez, L. del Campo, and M. J. Tello, *Int. J. Thermophys.* **29**, 1141 (2008).
- ³¹L. González-Fernández, R. B. Pérez-Sáez, L. del Campo, and M. J. Tello, *Appl. Opt.* **49**, 2728 (2010).
- ³²L. del Campo, R. B. Pérez-Sáez, L. González-Fernández, and M. J. Tello, *J. Appl. Phys.* **107**, 113510 (2010).
- ³³L. del Campo, R. B. Pérez-Sáez, M. J. Tello, X. Esquisabel, and I. Fernández, *Int. J. Thermophys.* **27**, 1160 (2006).

- ³⁴L. González-Fernández, E. Risueño, R. B. Pérez Sáez, and M. J. Tello, *J. Alloys Compd.* **541**, 144 (2012).
- ³⁵R. A. Matula, *J. Phys. Chem. Ref. Data* **8**, 1147 (1979).
- ³⁶K. L. F. Bane, G. Stupakov, and J. J. Tu, *Proceedings of European Particle Accelerator Conference (THPCH073)* (2006).
- ³⁷H. E. Bennett and J. M. Bennett, *Optical Properties and Electronic Structure of Metals and Alloys*, edited by F. Abeles (North-Holland, Amsterdam, 1966), p. 175.
- ³⁸M. A. Ordal, R. J. Bell, R. W. Alexander, L. A. Newquist, and M. R. Query, *Appl. Opt.* **27**, 1203 (1988).
- ³⁹M. A. Havstad and S. A. Self, *Int. J. Thermophys.* **14**, 1077 (1993).
- ⁴⁰S. Edalatpour and M. Francoeur, *J. Quant. Spectrosc. Radiat. Transfer* **118**, 75 (2013).
- ⁴¹M. F. Modest, *Radiative Heat Transfer* (Academic Press, 2003).
- ⁴²R. Siegel and J. Howell, *Thermal Heat Transfer*, 4th ed. (Taylor & Francis, Washington, 2002).